Electronic Supplementary Material (ESI) for Energy & Environmental Science.
This journal is © The Royal Society of Chemistry 2016

Electronic Supplementary Information

A dual-metal-organic-frameworks derived electrocatalyst for oxygen reduction

*Bu Yuan Guan, Le Yu and Xiong Wen (David) Lou**

School of Chemical and Biomedical Engineering, Nanyang Technological University,

62 Nanyang Drive, Singapore, 637459, Singapore

E-mail: xwlou@ntu.edu.sg; davidlou88@gmail.com

Webpage: http://www.ntu.edu.sg/home/xwlou/

Experimental details

Synthesis of MIL-88B@ZIF-8 dual-MOFs composites. The MIL-88B nanorods are synthesized according to the previously reported hydrothermal method. Briefly, 0.16 g of F127 is dissolved in 15 ml of deionized water, and 0.179 g of $FeCl_3 \cdot 6H_2O$ is added to the surfactant solution. The resulting solution is stirred for 1 h before 0.6 ml of acetic acid is injected. After the mixture is stirred for another hour, 0.06 g of 2-aminoterephthalic acid is added. The reaction mixture is stirred for another 2 h. Afterwards, the mixture is transferred into an autoclave and crystallized for 24 h at 110 ^{o}C. The dark brown product is recovered and washed with ethanol several times. Then the as-prepared MIL-88B nanorods are dispersed in 10 ml of methanol solution of PVP (0.5 g, M_w = 40000), and the mixture is further stirred at room temperature for 12 h. The PVP-functionalized MIL-88B nanorods are collected by centrifugation, washed by methanol several times, and

dispersed in 15 ml of methanol for further use. To synthesize MIL-88B@ZIF-8 dual-MOFs composites, 0.3 ml of MIL-88B nanorods suspension, 3 ml of 25 mM 2-MIM solution, 5 ml of 25 mM $Zn(NO_3)_2 \cdot 6H_2O$ solution, and 2.7 ml of methanol are mixed and then allowed to react at room temperature for 24 h without stirring. The product is then collected by centrifugation, washed with methanol several times, and vacuum dried overnight.

Synthesis of Fe_3C@N-CNT assemblies. The obtained MIL-88B@ZIF-8 dual-MOFs composite is placed in a ceramic boat, heated to 200 ^oC at a ramp rate of 5 ^oC min^{-1} and maintained for 2 h in a tube furnace under nitrogen atmosphere. The temperature in the furnace is further raised to 900 ^oC at a ramp rate of 5 ^oC min^{-1} and kept at that temperature for 2 h. After that, the furnace is cooled down to room temperature naturally.

Materials characterization. Field-emission scanning electron microscope (FESEM; JEOL-6700F) and transmission electron microscope (TEM; JEOL, JEM-2010) are used to examine the morphology and structure of the samples. The composition of the sample is analyzed by energy-dispersive X-ray spectroscopy (EDX) attached to the FESEM instrument. The crystal phase of the products is examined by X-ray diffraction (XRD) on a Bruker D2 Phaser X-Ray Diffractometer. Raman spectrum is recorded on a Renishaw InVia Reflex Raman microscope with an excitation laser of 514 nm. The nitrogen sorption isotherms are measured on a Quantachrome Autosorb AS-6B system.

Electrochemical measurements. The electrochemical measurements are carried out on glassy carbon disk with 5 mm in diameter that is polished with 0.05-micron alumina paste and then sonicated in distilled water and ethanol. Catalyst inks are prepared by dispersing 1 mg of catalyst materials (i.e., Fe_3C@N-CNT assemblies, Fe_3C-Fe/N-CNT mixture, porous carbon nanoshells, or 20 wt.% Pt/C catalyst) in the mixture of isopropanol (0.2 ml) and Nafion (5 wt.%, 10 μl). The ink solution is then sonicated for 30 min to get a uniform suspension. Then, 10 μl of the catalyst ink is deposited on the glassy carbon substrate to obtain a loading of 0.25 mg cm^{-2}. Platinum plate (1 cm^2) and saturated calomel electrode (SCE) are selected as the counter electrode and reference electrode, respectively. All potentials in this study are measured against the SCE reference electrode and converted to the reversible hydrogen electrode (RHE) reference scale by $E_{(RHE)} = E_{(SCE)} + 0.059pH + 0.242$. The electrochemical measurements are carried out at room temperature in a conventional three-electrode cell with 0.1 M KOH solution using a rotating disk electrode (RDE) setup from Pine Instrument Company connected to an Autolab potentiostat/galvanostat (Model PGSTAT-72637) workstation. The working electrode is scanned in 0.1 M KOH solution by CV at 20 mV s^{-1} and line sweep voltammetry (LSV) at 10 mV s^{-1}. Before CV and RDE tests, the 0.1 M KOH solution is bubbled with oxygen for 30 min. The current densities in both CV and RDE data are normalized to the geometric area (0.196 cm^2) of the glassy carbon disk.

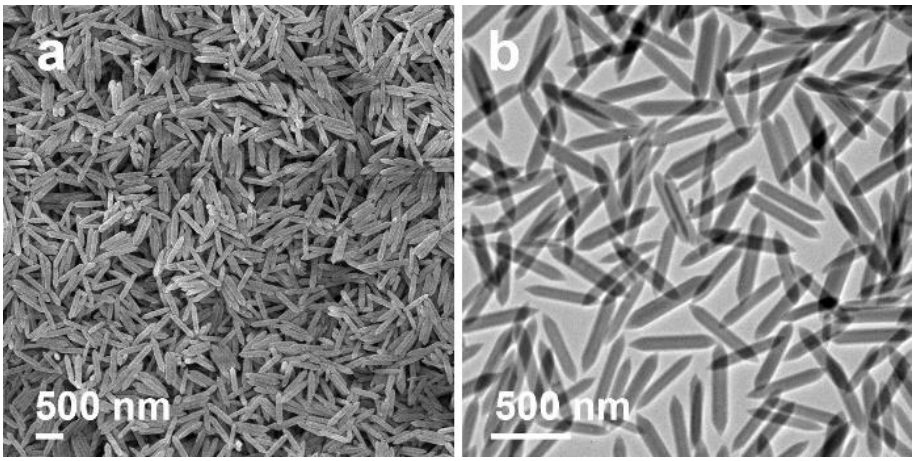

Fig. S1 FESEM (a) and TEM (b) images of as-prepared MIL-88B nanorods.

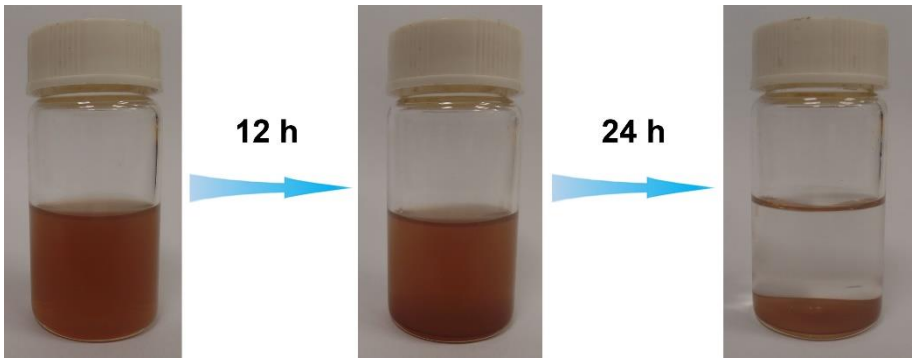

Fig. S2 Photographs of the mixed solution for the preparation of MIL-88B@ZIF-8 dual-MOFs.

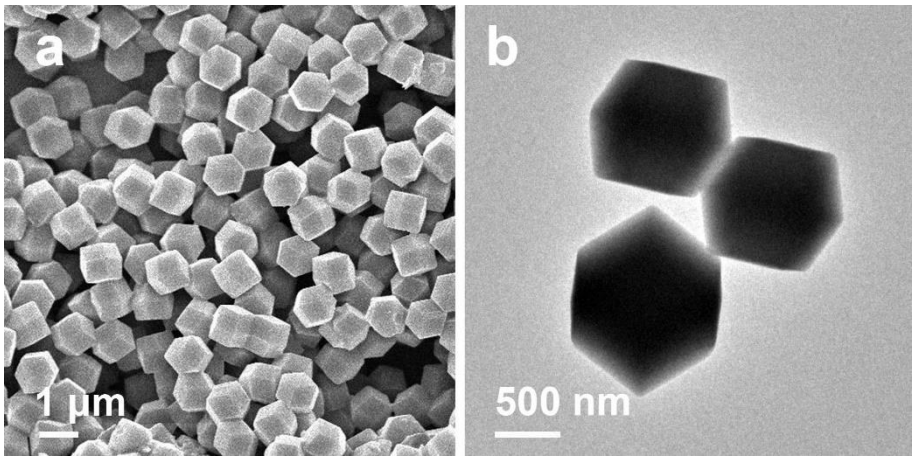

Fig. S3 FESEM (a) and TEM (b) images of ZIF-8 crystals.

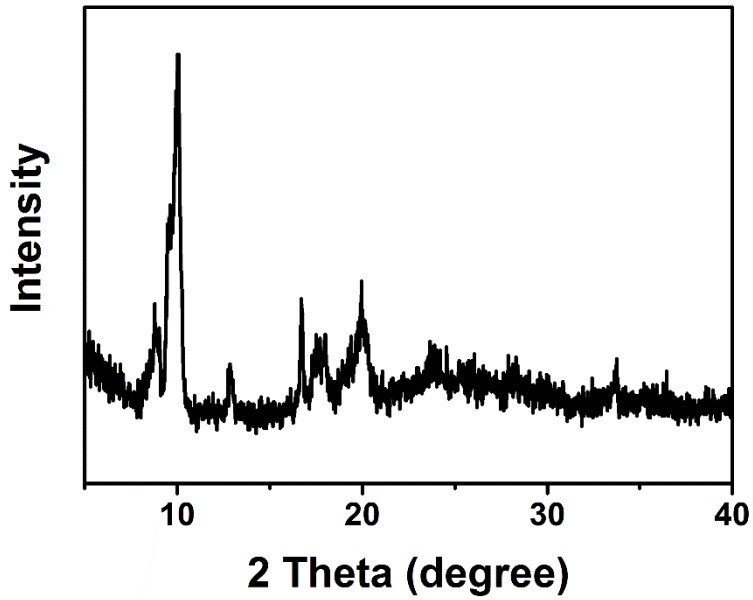

Fig. S4 XRD pattern of MIL-88B nanorods.

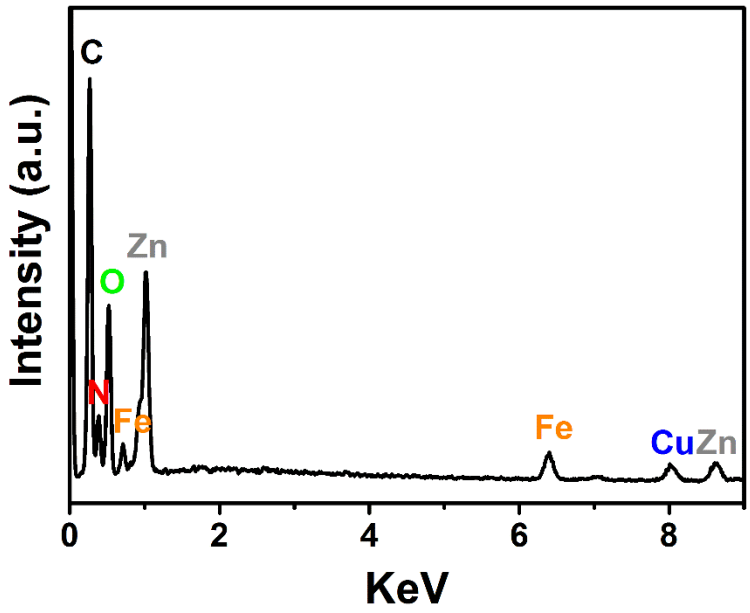

Fig. S5 EDX analysis of MIL-88B@ZIF-8 dual-MOFs.

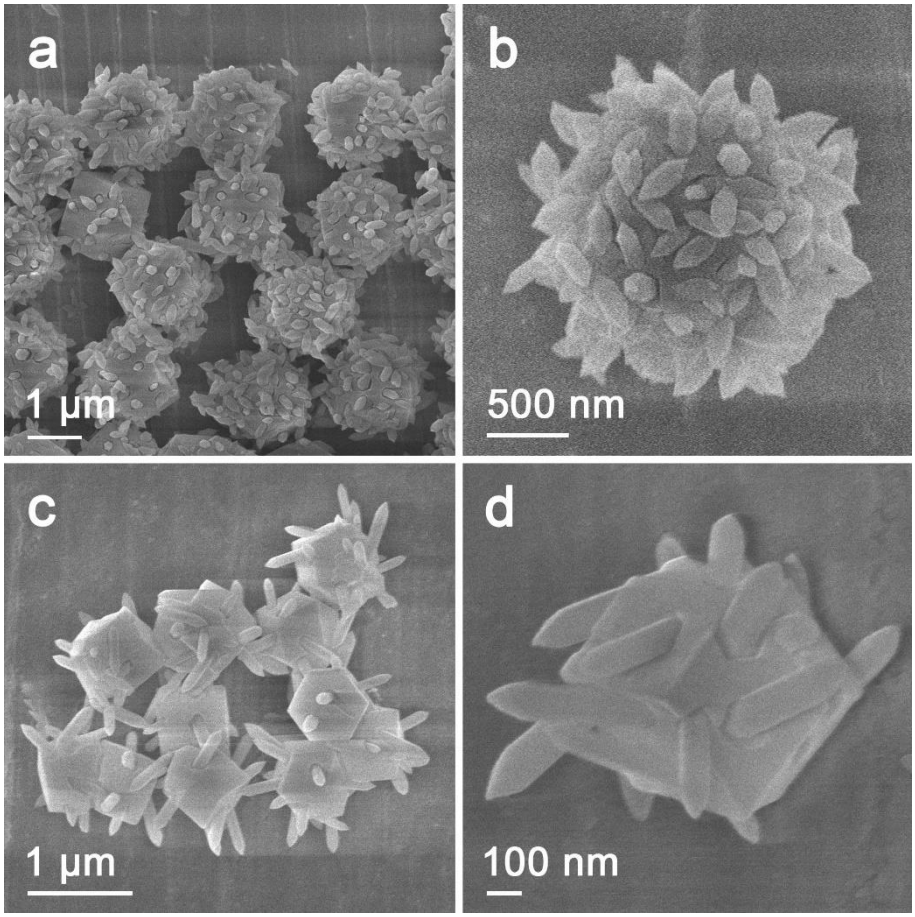

Fig. S6 FESEM images of MIL-88B@ZIF-8 dual-MOFs with (a, b) shorter MIL-88B nanorods and (c, d) fewer MIL-88B nanorods in each ZIF-8 crystal.

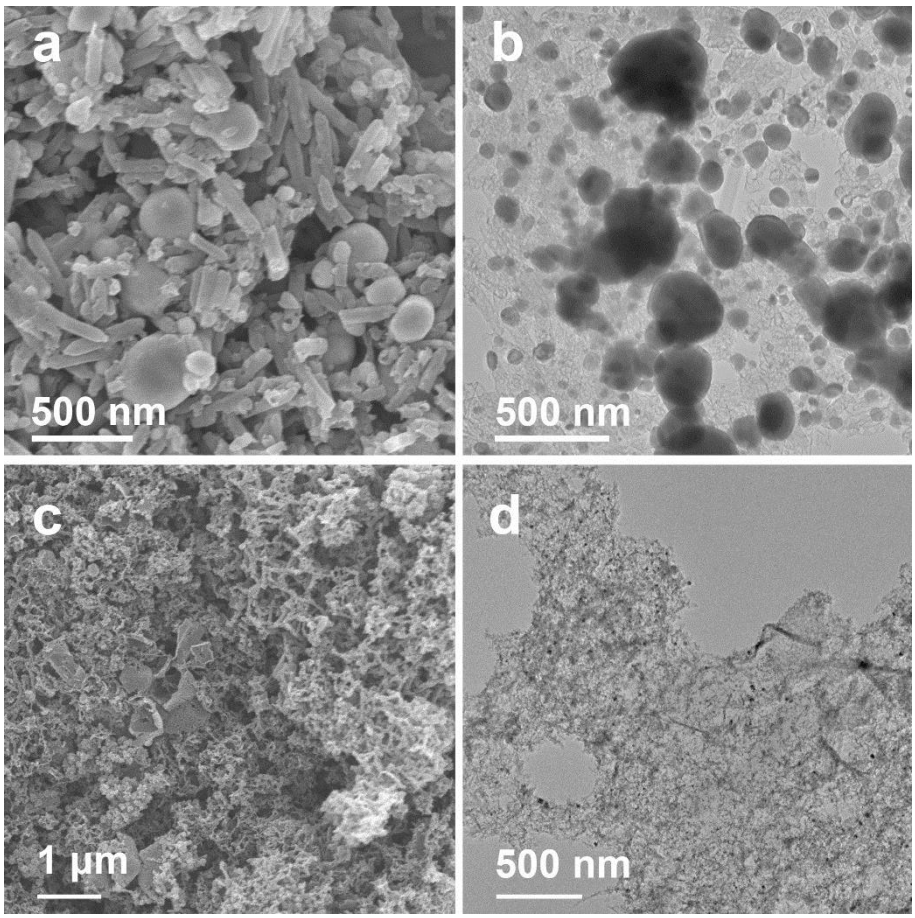

Fig. S7 FESEM and TEM images of (a, b) a mixture of strongly aggregated large Fe_3C partcles and empty N-CNTs derived from pyrolysis of MIL-88B nanorods and (c, d) cracked porous carbon nanoshells derived from pyrolysis of ZIF-8 crystals.

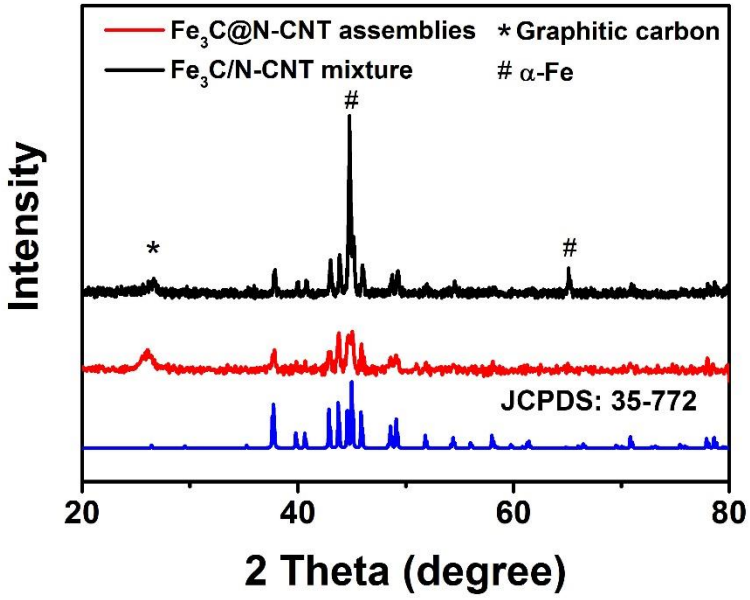

Fig. S8 XRD patterns of Fe_3C@N-CNT assemblies and Fe_3C-Fe/N-CNT mixture.

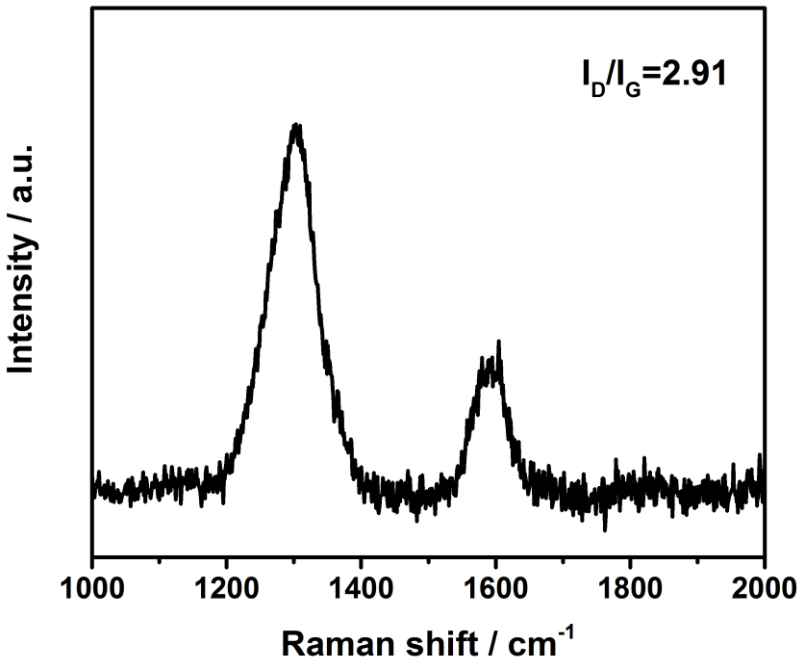

Fig. S9 Raman spectrum of the Fe_3C@N-CNT assemblies.

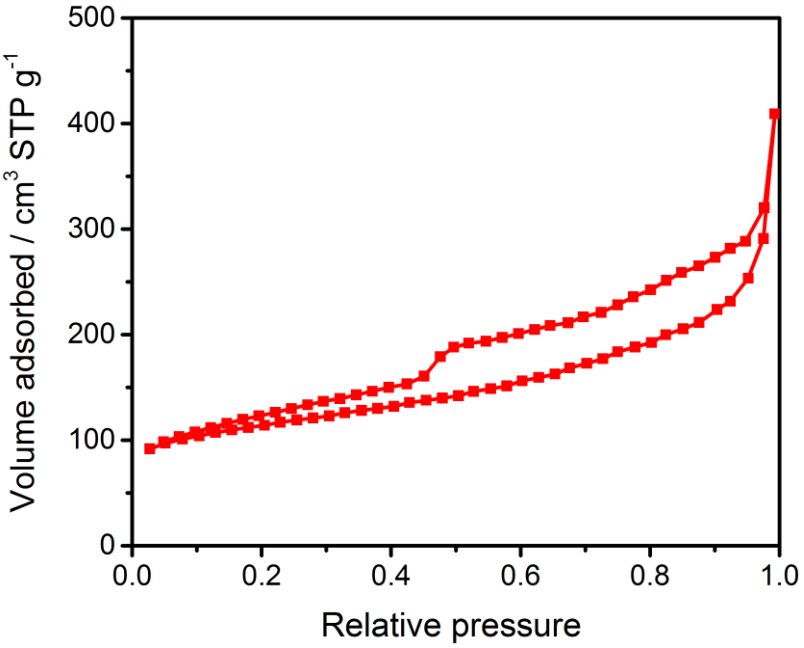

Fig. S10 N_2 adsorption-desorption isotherms of the Fe_3C@N-CNT assemblies.

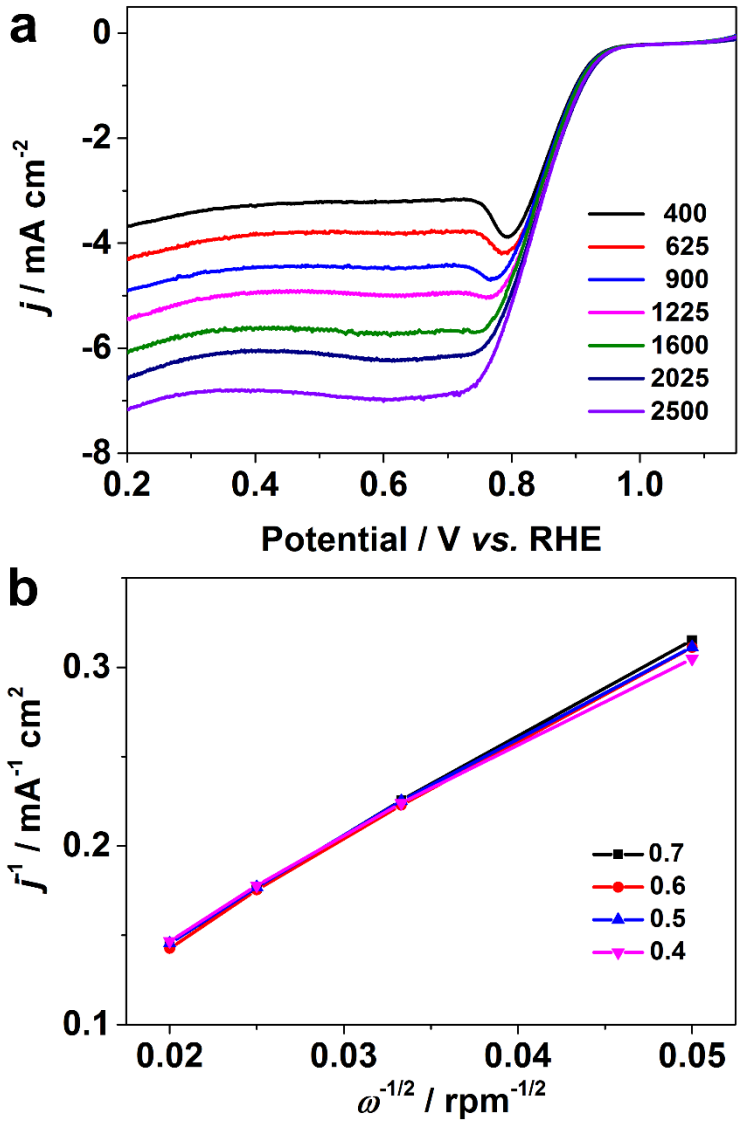

Fig. S11 (a) Line sweep voltammetry (LSV) curves of Fe_3C@N-CNT assemblies in O_2-saturated 0.1 M KOH solution with a sweep rate of 10 mV s^{-1} at different rotating speeds ranging from 400 to 2500 rpm. (b) Corresponding Koutecky-Levich plots (j^{-1} *vs.* $\omega^{-1/2}$) at different potentials from 0.4 to 0.7 V from the LSV curves shown in (a).

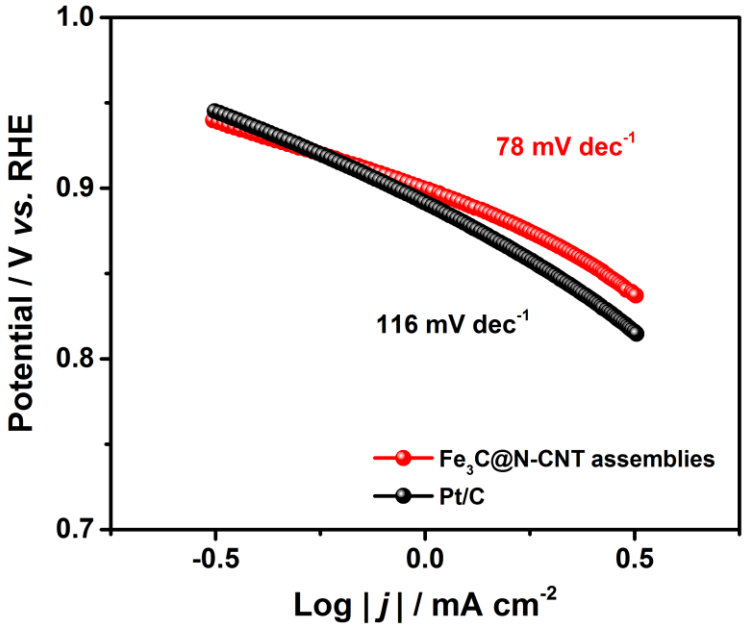

Fig. S12 Tafel plots of the Fe_3C@N-CNT assemblies and Pt/C catalyst.

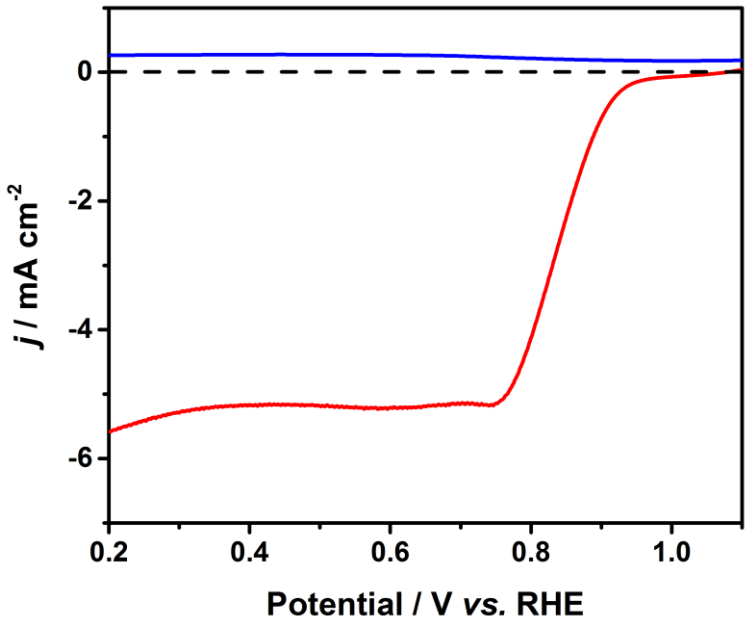

Fig. S13 Rotating ring-disk electrode (RRDE) curves at rotating speed of 1600 rpm with a sweep rate of 10 mV s^{-1}.

Table S1. Summary of various carbon-based electrocatalysts for ORR.

Catalyst	Onset potential (V)	Half-wave potential (V)	CV peak potential (V)	n	Reference
Fe/carbon fibers	0.91	0.81	N/A	4	*Science* **2011**, 332, 443
Co/graphene sheets	0.80	0.75	N/A	N/A	*Science* **2011**, 332, 443
VNCNT arrays	N/A	N/A	0.77	3.9	*Science* **2009**, 323, 760
CNT/graphene hybrid	0.89	0.76	0.75	4	*Nat. Nanotech.* **2012**, 7, 394
Co_3O_4/graphene sheets	0.88	0.83	0.84	3.9	*Nat. Mater.* **2011**, 10, 780
N-CNT frameworks	0.97	0.87	0.87	3.97	*Nat. Energy* 2016, 1, 15006
Mesoporous N-doped carbon	0.978	0.85	0.83	3.97	*Nat. Commun.* **2014**, 5, 5974
N-CNT/carbon nanoparticle	1.08	0.87	N/A	3.92	*Nat. Commun*. **2013**, 4, 1922
FeN_x/carbon composite	0.94	0.82	N/A	N/A	*J. Am. Chem. Soc.* **2014**, 136, 10882
Fe/N-doped carbon	0.92	0.80	0.85	3.96	*J. Am. Chem. Soc.* **2014**, 136, 1102
N-doped carbon frameworks	0.79	0.79	N/A	3.95	J. Am. Chem. Soc. **2013**, 135, 16002
graphene-MOF composite	0.91	N/A	0.74	3.82	*J. Am. Chem. Soc.* **2012**, 134, 6707
N-doped hollow fibers	0.75	0.83	0.77	3.6	*J. Am. Chem. Soc.* **2014**, 136, 14385
N, P-doped hollow fibers	0.9	0.71	0.77	4.0	*J. Am. Chem. Soc.* **2014**, 136, 14385
ZIF-derived porous carbon polyhedra	0.83	N/A	0.68	3.3	*J. Am. Chem. Soc.* **2014**, 136, 6790
CNTs/carbon hybrid	0.92	0.82	N/A	3.8	*Angew. Chem. Int. Ed.* **2014**, 53, 4102
Graphene/Co_3O_4 sheets	0.95	N/A	N/A	3.9	*Angew. Chem. Int. Ed.* **2013**, 52, 12105
N-doped graphene/metal sheets	0.94	N/A	0.67	3.95	*Angew. Chem. Int. Ed.* **2014**, 53, 1570

COF-derived metal-doped carbon sheets	0.90	N/A	0.77	3.61	*Angew. Chem. Int. Ed.* **2014**, 53, 2433
ZIF-derived porous carbon/graphene	0.95	N/A	0.82	3.98	*Angew. Chem. Int. Ed.* **2014**, 53,14235
P-doped ordered mesoporous carbon	0.92	0.82	0.72	3.5	*Angew. Chem. Int. Ed.* **2015**, 54,9230
N,P-codoped ordered mesoporous carbon	0.95	0.82	0.73	3.7	*Angew. Chem. Int. Ed.* **2015**, 54,9230
Ordered mesoporous carbon	0.81	0.69	N/A	3.1	*Angew. Chem. Int. Ed.* **2015**, 54,9230
sulphur-doped graphene	0.88	0.66	0.69	3.13	*Angew. Chem. Int. Ed.* **2015**, 54,1888
Fe/bamboo-like N-CNTs	N/A	N/A	0.74	N/A	*Adv. Mater.* **2014**, 26, 6074
ZIF-derived porous carbon	0.9	0.76	N/A	3.9	*Adv. Mater.* **2014**, 26, 1093
P-doped graphene	0.91	N/A	0.58	3.8	*Adv. Mater.* **2013**, 25, 4932
N-doped graphene/Co porous carbon polyhedra	0.97	0.86	0.82	3.9	*Adv. Funct. Mater.* **2015**, *25,* 872
N-doped Co/graphene porous carbon	0.94	N/A	0.80	3.3	*Adv. Funct. Mater.* **2015**, *25,* 872
Metal/N-doped carbon	0.97	0.82	0.78	3.97	*ChemElectroChem* **2015**, *2*, 2089
N-doped hierarchical porous carbon	0.9	0.78	0.7	3.2	*Carbon* **2015**, 86,108
Co/N-carbon fibers	0.95	N/A	0.85	3.9	*Chem. Eur. J.* **2015**, *21,* 2165
Fe_3C@N-CNT assemblies	0.97	0.85	0.83	3.96	This work